INSTITUTE OF PHYSICS PUBLISHING JOURNAL OF PHYSICS: CONDENSED MATTER

J. Phys.: Condens. Matter **16** (2004) 7225–7232 PII: S0953-8984(04)81845-9

Misfit dislocation loops in cylindrical quantum dots

I A Ovid'ko and A G Sheinerman

Institute of Problems of Mechanical Engineering, Russian Academy of Sciences, Bolshoj 61, Vasilyevsky Ostrov, St Petersburg 199178, Russia

E-mail: ovidko@def.ipme.ru

Received 8 June 2004, in final form 6 August 2004
Published 1 October 2004
Online at stacks.iop.org/JPhysCM/16/7225
doi:10.1088/0953-8984/16/41/005

Abstract

A theoretical model is suggested which describes the generation of prismatic misfit dislocation loops surrounding cylindrical quantum dots. These dislocation loops partly accommodate misfit stresses in cylindrical quantum dots embedded in a film deposited onto a substrate. In the framework of the model, the ranges of geometric parameters (misfit parameter f, quantum dot radius a and its height H) are calculated at which the generation of misfit dislocation loops surrounding cylindrical quantum dots is energetically favourable. The exemplary cases of dislocation loop generation in $In_xGa_{1-x}N$/GaN and GaN/AlN systems are briefly discussed.

1. Introduction

Semiconductor quantum dots represent the subject of intense fundamental and applied research efforts motivated by wide perspectives of their application in optoelectronics, see, e.g. [1–3]. The functional properties of quantum dots are highly sensitive to their spatial arrangement, shape and structure. Therefore, there are certain demands on fabrication of quantum dot ensembles to be exploited in nanodevices. One of the prospective methods to produce spatially ordered ensembles of quantum dots which are uniform in both size and shape, highly desirable for applications, is the fabrication through a selective growth process that consists of deposition of a thin layer on a substrate and its subsequent patterning with sub-micron holes [4, 5]. Quantum dots are then selectively grown inside the holes using a variety of techniques, such as metal–organic vapour deposition and molecular beam epitaxy. In doing so, cylindrical quantum dots (figure 1) are fabricated which commonly have very similar sizes and shapes controlled by the geometry of the holes in the layer mask [4, 5]. However, in the case under consideration, the misfit dislocations in cylindrical quantum dots can be formed to accommodate the misfit stresses (arising in both the substrate and the dots due to the misfit between their crystal lattices), as with conventional pyramidal and dome-like quantum dots [1, 6–10] fabricated by self-assembly based techniques. The generation of misfit dislocations leads to a dramatic

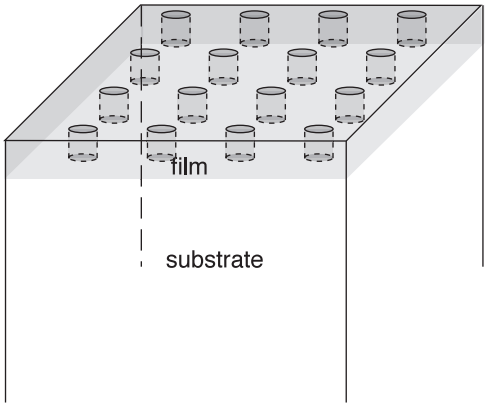

Figure 1. Cylindrical quantum dots embedded into a film deposited onto a substrate.

degradation of the functional optoelectronic properties of quantum dots [1]. In this context, it is very important to identify the critical geometric parameters of cylindrical quantum dots, at which the generation of misfit dislocations is energetically favourable. In analysis of misfit dislocations in pyramidal and dome-like quantum dots and conventional continuous films, straight misfit dislocations and their configurations are commonly considered; see, e.g., [6–15]. However, with the geometry of cylindrical quantum dots, it is natural to think that misfit dislocation loops can be intensively formed which surround these cylindrical quantum dots. Recently, the conditions for the formation of misfit dislocation loops around spherical quantum dots in a matrix [16] and in a film on a substrate [17] have been theoretically analysed. The main aim of this paper is to suggest a theoretical model which describes the generation of prismatic misfit dislocation loops surrounding cylindrical quantum dots. The focus will be placed on calculations of the ranges of geometric parameters at which the generation of misfit dislocation loops in cylindrical quantum dots is energetically favourable.

2. Model

Let us consider a cylindrical quantum dot embedded into a film of thickness t deposited onto a substrate (figure 2). The central axis of the cylindrical quantum dot is perpendicular to the film free surface, and the upper surface of the dot enters the film free surface (figure 2). We consider the situation where the atomic bonding at the interphase boundary between the adjacent film and quantum dot lattices is strong. In the framework of this model approximation, in the following, we consider a cylindrical second-phase inclusion with the radius a and height $H \leqslant t$ in a film on a semi-infinite substrate. The central axis of the cylindrical inclusion is perpendicular to the film free surface, and the upper surface of the inclusion enters the film free surface (figure 2). The substrate, film and inclusion are assumed to be elastically isotropic solids having the same values of the shear modulus G and the same values of the Poisson ratio ν. The difference between the crystal lattice parameters, a_s and a_f, of the matrix and film is characterized by the misfit $\tilde{f} = (a_s - a_f)/a_f$, while the difference between the crystal lattice parameters, a_f and a_i, of the film and inclusion is characterized by the misfit $f = (a_f - a_i)/a_i$. It is important to note that the parameter f defines here the misfit between the inclusion and the film but not between the inclusion and the substrate.

The elastic misfit strains and stresses occur in the matrix, film and inclusion due to the misfits f and $\tilde{f}$ at the interphase boundaries. These strains and stresses provide the coherent matching of the crystal lattices of the adjacent phases. In certain ranges of parameters that

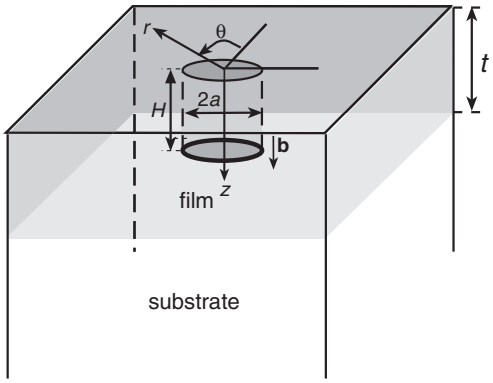

Figure 2. Misfit dislocation loop around a cylindrical quantum dot situated within a film on a substrate. The loop is shown as a solid circle.

characterize the matrix–film–inclusion composite system, the misfit stresses are partly relaxed through the generation of misfit defects at the interphase boundaries. In this paper, we consider the defect configuration which is typical for cylindrical solids and provides effective relaxation of the misfit stresses. It is a prismatic misfit dislocation loop surrounding the cylindrical quantum dot (figure 2). Such a misfit dislocation loop can be generated at the film free surface and then move (glide) towards the cylinder bottom where the loop provides the most effective relaxation of the misfit stresses.

3. Energy characteristics of misfit dislocation loop

In order to reveal the conditions for the energetically favourable formation of a misfit dislocation loop surrounding a cylindrical quantum dot (figure 2), let us introduce the cylindrical coordinate system (r, θ, z) as shown in figure 2. In this coordinate system, the line of the dislocation loop has the coordinates $(r = a, z = H)$, and the Burgers vector $\boldsymbol{b}$ of the dislocation loop is written as $b_z \boldsymbol{e}_z$.

The energy change related to the formation of the misfit dislocation loop is given as $\Delta W = W^l + W^{l-f} + W^{l-\tilde{f}} + W^{\mathrm{c}}$. Here W^l is the proper elastic energy of the misfit dislocation loop, W^{l-f} and $W^{l-\tilde{f}}$ are the energies of the interaction between the dislocation loop and the stresses created due to the misfits f and $\tilde{f}$, respectively, and W^{c} is the dislocation core energy. The formation of a misfit dislocation loop surrounding the cylindrical quantum dot shown in figure 2 is energetically favourable, if the characteristic energy change is negative, that is,

$$\Delta W = W^l + W^{l-f} + W^{l-\tilde{f}} + W^{\mathrm{c}} < 0. \tag{1}$$

Let us consider the terms figuring on the right-hand side of formula (1). The proper elastic energy W^l of the dislocation loop can be calculated with the help of formulas (9), (12) and (13) given in paper [18]. In doing so, we have $W^l = Gb^2 a Q/[2(1-\nu)]$. Here b is the Burgers vector magnitude of the dislocation loop and

$$Q = \ln \frac{8a}{r_0} - 2 + \frac{k}{2}\left[(k^2-3)K(k) - (2k^2-3)E(k)\right], \tag{2}$$

where r_0 is the dislocation core radius, $k = (\xi_0^2 + 1)^{-1/2}$, $\xi_0 = H/a$, while $K(k) = \int_0^{\pi/2}(1-\sin^2\varphi)^{-1/2}\,\mathrm{d}\varphi$ and $E(k) = \int_0^{\pi/2}(1-\sin^2\varphi)^{1/2}\,\mathrm{d}\varphi$ are the complete elliptic integrals of the first and second kind, respectively.

The energy W^{l-f} of the interaction between the misfit dislocation loop and misfit stresses created by the quantum dot is calculated with the help of the following general formula [19]:

$$W^{l-f} = f\int_0^{2\pi} \mathrm{d}\theta \int_0^a r\,\mathrm{d}r \int_0^H \mathrm{d}z\,(\sigma_{rr}^l + \sigma_{\theta\theta}^l + \sigma_{zz}^l), \tag{3}$$

where σ_{rr}^l, $\sigma_{\theta\theta}^l$ and σ_{zz}^l are the stress tensor components of the misfit dislocation loop shown in figure 2. The stress field of such a loop has been calculated in papers [18, 20]. However, the formulas given in these papers contain misprints. After revision, we have the correct versions of these formulas for the non-zero components of the dislocation loop stress field (in units of $Gb_z/[2(1-\nu)a]$) to be as follows:

$$\begin{aligned}\sigma_{rr}^l = {} & -J_1(1,0;1) + \frac{1-2\nu}{\rho}J_1(1,1;0) + |\xi-\xi_0|\left(J_1(1,0;2) - \frac{J_1(1,1;1)}{\rho}\right) + J_2(1,0;1) \\ & - (\xi - 3\xi_0)J_2(1,0;2) + \frac{1}{\rho}[(2\nu-1)J_2(1,1;0) \\ & + (\xi - (3-4\nu)\xi_0)J_2(1,1;1)] - 2\xi_0\xi\left(J_2(1,0;3) - \frac{J_2(1,1;2)}{\rho}\right),\end{aligned} \tag{4}$$

$$\begin{aligned}\sigma_{\theta\theta}^l = {} & -2\nu J_1(1,0;1) - \frac{1-2\nu}{\rho}J_1(1,1;0) + |\xi-\xi_0|\frac{J_1(1,1;1)}{\rho} + 2\nu J_2(1,0;1) \\ & + 4\nu\xi_0 J_2(1,0;2) - \frac{1}{\rho}\left[(2\nu-1)J_2(1,1;0) + (\xi-(3-4\nu)\xi_0)J_2(1,1;1)\right] \\ & - 2\xi_0\xi\frac{J_2(1,1;2)}{\rho},\end{aligned} \tag{5}$$

$$\sigma_{zz}^l = -J_1(1,0;1) - |\xi-\xi_0|J_1(1,0;2) + J_2(1,0;1) + (\xi+\xi_0)J_2(1,0;2) + 2\xi_0\xi J_2(1,0;3), \tag{6}$$

$$\sigma_{rz} = -(\xi-\xi_0)J_1(1,1;2) + (\xi-\xi_0)J_2(1,1;2) + 2\xi_0\xi J_2(1,1;3). \tag{7}$$

Here $\rho = r/a$, $\xi = z/a$, $J_{1,2}(m,n;p) = \int_0^\infty J_m(t)J_n(\rho t)\mathrm{e}^{-|\xi\mp\xi_0|t}t^p\,\mathrm{d}t$ are the Lipschitz–Hankel integrals [21]. The stress tensor components given by the expressions (4)–(7) obey both the equilibrium equations and the boundary conditions at the free surface $z = 0$.

With the expressions (4)–(6) substituted into formula (3), after integration in this formula, we find $W^{l-f} = -[8\pi G(1+\nu)a^2 b_z f/(1-\nu)]M$, where

$$\begin{aligned}M = {} & \frac{1}{32\xi_0^2}\big\{8F(1/2,1/2;2;-4/\xi_0^2)\xi_0^2 - 4F(1/2,1/2;2;-1/\xi_0^2)\xi_0^2 \\ & - 8F(3/2,3/2;3;-4/\xi_0^2) + F(3/2,3/2;3;-1/\xi_0^2)\big\},\end{aligned} \tag{8}$$

$F(\alpha,\beta;\gamma;x)$ is the hypergeometric series given by definition as follows:

$$F(\alpha,\beta;\gamma;x) = \frac{\Gamma(\gamma)}{\Gamma(\alpha)\Gamma(\beta)}\sum_{k=0}^{\infty}\frac{\Gamma(\alpha+k)\Gamma(\beta+k)}{\Gamma(\gamma+k)}\frac{x^k}{k!}. \tag{9}$$

Here $\Gamma(t)$ is the gamma-function.

The energy $W^{l-\tilde{f}}$ of the interaction between the dislocation loop and the misfit stresses $\sigma_{ij}^{\tilde{f}}$ acting within the film and quantum dot due to the misfit $\tilde{f}$ is given as [19]

$$W^{l-\tilde{f}} = -\int_V \beta_{ij}^{*l}\sigma_{ij}^{\tilde{f}}\,\mathrm{d}V', \tag{10}$$

where $i, j = r, \theta, z$, β_{ij}^{*l} is the plastic distortion induced by the dislocation loop, and integration is performed over the entire volume V of the matrix–film–inclusion composite. In formula (10),

the summation over the repeated indices is carried out. In the situation under consideration (figure 2), there are only the following non-zero components of the misfit stress tensor $\sigma_{ij}^{\tilde{f}}$:

$$\sigma_{rr}^{\tilde{f}} = \sigma_{\theta\theta}^{\tilde{f}} = \frac{2G(1+\nu)\tilde{f}}{1-\nu}\Theta(t-z), \tag{11}$$

where $\Theta(x)$ is the Heavyside function, equal to 1 for $x > 0$, and to 0 for $x < 0$. At the same time, there is only the following non-zero component of the plastic distortion tensor β_{ij}^{*l} created by the dislocation loop [19]:

$$\beta_{zz}^{*l} = b_z\Theta(a-r)\delta(z-H), \tag{12}$$

where $\delta(z-H)$ is the Dirac delta-function. The substitution of the expressions for $\sigma_{ij}^{\tilde{f}}$ and β_{ij}^{*l} into formula (10) yields $W^{l-\tilde{f}} = 0$. This means that the examined dislocation loop does not interact with the misfit stresses $\sigma_{ij}^{\tilde{f}}$. As a corollary, the conditions for the dislocation loop generation do not depend on the value of the misfit $\tilde{f}$.

The dislocation core energy W^{c} figuring in inequality (1) is given by the standard approximate formula [22]: $W^{\mathrm{c}} \approx Gb^2l/[4\pi(1-\nu)]$. Here $l = 2\pi a$ is the length of the dislocation loop.

4. Criterion for energetically favourable formation of misfit dislocation loop

Substitution of the expressions for W^l, W^{l-f}, $W^{l-\tilde{f}}$ and W^{c} into inequality (1) yields the following criterion for the energetically favourable formation of the misfit dislocation loop surrounding the cylindrical quantum dot (figure 2): $|f| > f_{\mathrm{c}}$, where

$$f_{\mathrm{c}} = \frac{(Q+1)b}{16\pi(1+\nu)aM}. \tag{13}$$

The parameter f_{c} figuring on the left-hand side of formula (13) represents the critical misfit for the energetically favourable formation of the misfit dislocation loop with the Burgers vector projection (on the z-axis) being either $b_z = b$ (if $f > 0$) or $b_z = -b$ (if $f < 0$). The critical misfit f_{c}, given by (13), is a function of two variables, a/b and H/b (see figure 3).

The dependences of the critical misfit f_{c} on the dimensionless quantum dot radius a/b are presented in figure 3(a), for $\nu = 0.3$, $r_0 = b$ and various values of the quantum dot height H. As follows from figure 3(a), for any finite value of H, each of the dependences $f_{\mathrm{c}}(a/b)$ has a sole minimum at $a \approx H/2$. If $|f|$ is lower than the minimum value of $f_{\mathrm{c}}(a/b)$ at given value of H, the formation of the misfit dislocation loop is energetically unfavourable at any a. If $|f|$ is larger than the minimum value of the function $f_{\mathrm{c}}(a/b)$, there is a range of a in which the formation of the misfit dislocation loop is energetically unfavourable. For a given value of a and $|f| < f_{\mathrm{c}}(H \to \infty)$, the generation of misfit dislocation loops is energetically unfavourable at any height H of a quantum dot.

The dependences $f_{\mathrm{c}}(H/b)$, for $\nu = 0.3$, $r_0 = b$ and various values of the quantum dot radius a, are shown in figure 3(b). As follows from figure 3(b), the critical misfit f_{c} decreases with rising H and saturates in the limit of $H \to \infty$.

The contour map of the critical misfit f_{c} in the coordinate space $(a/b, H/b)$ is presented in figure 4, for $\nu = 0.3$ and $r_0 = b$. As follows from figures 3 and 4, the critical misfit f_{c} decreases when the quantum dot height H grows and/or the quantum dot diameter $2a$ approaches H. In contrast, when H decreases and/or the dot diameter changes so as to increase the difference $|2a - H|$, the critical misfit f_{c} grows, in which case the dislocation loop formation (figure 2) is hampered. The curves shown in figure 4 have vertical asymptotes $a = a_{\mathrm{c}}$. For a given value

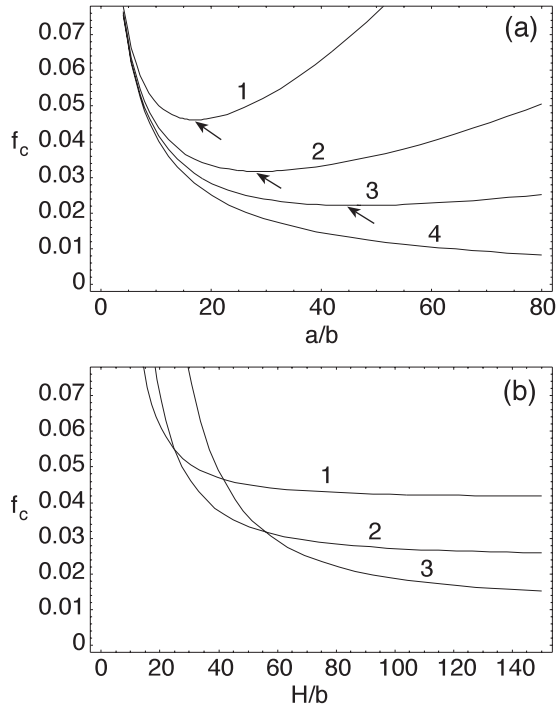

Figure 3. Dependences of critical misfit f_c on (a) non-dimensional radius a/b of quantum dot, for $H/b = 30$, 50, 80 and ∞ (curves 1, 2, 3 and 4, respectively) and (b) non-dimensional height H/b of quantum dot, for $a/b = 10$, 20 and 50 (curves 1, 2 and 3, respectively). The plots are drawn for $\nu = 0.3$ and $r_0 = b$. The arrows indicate the minima of curves 1, 2 and 3.

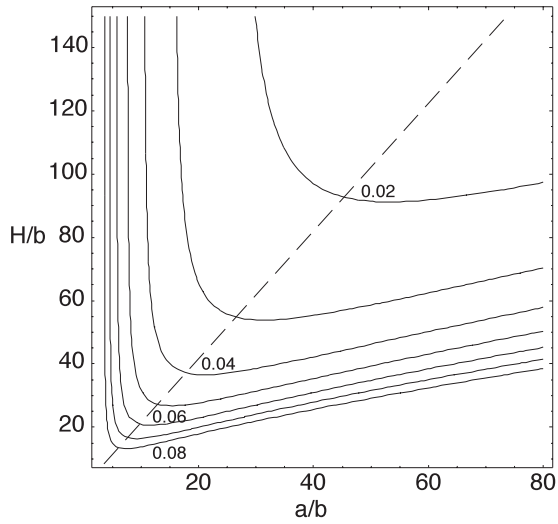

Figure 4. Contour map of critical misfit f_c in coordinate space $(a/b, H/b)$. The dashed line shows the line $a = H/2$.

of f and $a < a_c$, the generation of misfit dislocation loops is energetically unfavourable at any height H of a quantum dot. When f is given, a_c can be found from curve 4 shown in

figure 3(a). More precisely, the value $a = a_c$ corresponds to the point where this curve and the horizontal line $|f| = f_c$ intersect.

For illustration, let us give values of the critical radius a_c (that characterizes the energetically favourable generation of a misfit dislocation loop surrounding a cylindrical quantum dot; see figure 2) in several systems interesting for technological applications. For $In_{0.18}Ga_{0.82}N$/GaN system, $|f| = 0.02$. In this case, we have $a_c \approx 13$ nm at $b = 0.5$ nm. For the GaN/AlN system, $|f| = 0.027$, in which case we find $a_c \approx 8.5$ nm at $b = 0.5$ nm.

5. Concluding remarks

Thus, in this paper the new type of misfit defect configuration—a prismatic misfit dislocation loop surrounding a cylindrical quantum dot (figure 2)—has been theoretically examined. According to our theoretical analysis, the generation of misfit dislocation loops in composites with cylindrical quantum dots is crucially affected by their geometric parameters, such as misfit parameter f, quantum dot radius a and its height H. There are certain ranges of these parameters at which the generation of misfit dislocation loops surrounding cylindrical quantum dots (figure 2) is energetically favourable. In particular, one can distinguish both the critical misfit f_c (given by formula (13)) and critical radius a_c that characterize the energetically favourable formation of misfit dislocation loops. More precisely, the dislocation loop generation is favourable, if $|f| > f_c$. At the same time, in a composite system characterized by the misfit parameter f, the generation of misfit dislocation loops is energetically unfavourable at any height H of a quantum dot, if the quantum dot radius obeys the following inequality: $a < a_c$. The critical misfit f_c grows with a decrease in H and/or such a change of the dot radius a that leads to an increase in the absolute difference $|2a - H|$. These basic results of our theoretical analysis should be definitely taken into consideration in further experimental and theoretical study of cylindrical quantum dots, because of their fundamental significance and potential use in technological applications.

Also, notice that the model composite system shown in figure 2 is very similar to nanocomposite solids consisting of a matrix and carbon nanotubes. Such nanotube-reinforced composites exhibit the outstanding mechanical properties highly desirable for a wide range of structural applications; see, e.g., [23–25]. In this context, the theoretical results of our paper are worth being used in a description of the behaviour of dislocation loops surrounding carbon nanotubes in advanced nanotube-reinforced composites. This will be the subject of further investigations of the authors.

Acknowledgments

This work was supported, in part, by the Office of US Naval Research (grant N00014-01-1-1020), INTAS (grant 03-51-3779), the Russian Science Support Foundation, the Russian Academy of Sciences programme 'Structural mechanics of materials and construction elements', the Integration Programme (grant B 0026) St Petersburg Government (grant PD04-1.10-9) and St Petersburg Scientific Centre. Many thanks are due to Dr S Ganti for attracting our attention to cylindrical quantum dots as a promising class of wide bandgap nanostructures.

References

[1] Shchukin V A and Bimberg D 1999 *Rev. Mod. Phys.* **71** 1125–71

[2] Williams R S and Medeiros-Ribeiro G 2003 *Nanostructures: Synthesis, Functional Properties and Applications* ed T Tsakalakos, I A Ovid'ko and A K Vasudevan (Dordrecht: Kluwer) pp 81–93

[3] Teichert C 2002 *Phys. Rep.* **365** 335–432
[4] Tachibana K, Someya T, Ishida S and Arakawa Y 2002 *J. Cryst. Growth* **237** 1312–15
Tachibana K, Someya T, Satomi I and Arakawa Y 2000 *Appl. Phys. Lett.* **76** 3212–4
[5] Kawasaki K, Nakamatsu I, Hirayama H, Tsutsui K and Aoyagi Y 2002 *J. Cryst. Growth* **243** 129–33
[6] Johnson H T and Freund L B 1997 *J. Appl. Phys.* **81** 6081–90
[7] Kamins T I, Karr E C, Williams R S and Rosner S J 1997 *J. Appl. Phys.* **81** 211–9
[8] Pehlke E, Moll N, Kley A and Scheffler M 1997 *Appl. Phys.* A **65** 525–34
[9] Ovid'ko I A 2002 *Phys. Rev. Lett.* **88** 046103
[10] Ovid'ko I A and Sheinerman A G 2002 *Phys. Rev.* B **66** 245309
[11] Fitzgerald E A 1991 *Mater. Sci. Rep.* **7** 87–142
[12] van der Merve J H 1991 *Crit. Rev. Solid State Mater. Sci.* **17** 187–209
[13] Jain S C, Harker A H and Cowley R A 1997 *Phil. Mag.* A **75** 1461–515
[14] Gutkin M Yu, Ovid'ko I A and Sheinerman A G 2000 *J. Phys.: Condens. Matter* **12** 5391–401
Ovid'ko I A, Sheinerman A G and Skiba N V 2003 *J. Phys.: Condens. Matter* **15** 1173–81
[15] Ovid'ko I A and Sheinerman A G 2001 *J. Phys.: Condens. Matter* **13** 7937–51
Ovid'ko I A and Sheinerman A G 2003 *J. Phys.: Condens. Matter* **15** 2127–35
[16] Kolesnikova A L and Romanov A E 2003 *Tech. Phys. Lett.* **30** 126–8
[17] Kolesnikova A L and Romanov A E 2004 *Phys. Solid State.* **46** 1644–8
[18] Dundurs J and Salamon N J 1972 *Phys. Status Solidi* b **50** 125–33
[19] Mura T 1987 *Micromechanics of Defects in Solids* (Dordrecht: Martinus Nijhoff)
[20] Baštecká J 1964 *Czech. J. Phys.* B **14** 430–42
[21] Eason G, Noble B and Sneddon I N 1955 *Phil. Trans. R. Soc.* **247** 529–51
[22] Hirth J P and Lothe J 1982 *Theory of Dislocations* (New York: Wiley)
[23] Thostenson E T, Ren Z F and Chou T-W 2001 *Compos. Sci. Technol.* **61** 1899–912
[24] Thostenson E T and Chou T-W 2002 *J. Phys. D: Appl. Phys.* **36** 573–82
[25] Lau K T and Hui D 2002 *Composites* B **33** 263–70